Trabajo de fin de Grado

Implementation of Small Angle X-Ray Scattering technique for nanomaterials at Servicio Integrado de Difracción de Rayos X

Zaida Curbelo Cano

Tutorized by

Javier González Platas

Grado en Física | Facultad de Ciencias
Universidad de La Laguna

Julio de 2019

ABSTRACT

In this work we aim to implement Small Angle X-ray Scattering (SAXS) technique for nanomaterials at Servicio Integrado de Difracción de Rayos X (SIDIX), Universidad de La Laguna. We first reminded some basic notions on X-ray scattering and SAXS intensity contributions. Briefly, scattering profiles strongly depend on the averaged particle size and shape. The experimental setup is a diffractometer prepared for powder samples in a linear collimation system and surrounded by air. We have measured a set of verification samples whose mean particle radius and surface to volume ratio values validate the correct methodology. The data analysis process is based on gaussian and log-normal approximations for the size distribution curves. The results for the verification samples have been accurate, thus the experimental process and data analysis is correct. Furthermore, we applied the method into some real samples getting correct results for some of them. The main limitation of the followed method is the required hypothesis over particles structure and shape.

RESUMEN

El objetivo de este trabajo es implementar correctamente la técnica SAXS en el Servicio Integrado de Difracción de Rayos X (SIDIX) de la Universidad de La Laguna. Para comenzar hacemos alusión a nociones básicas sobre la dispersión de rayos X y las contribuciones a la intensidad de scattering en SAXS. Principalmente los perfiles de scattering tienen una gran dependencia con la forma y el tamaño promedio de las partículas. En la configuración experimental se utilizará un difractómetro de polvo, en un sistema óptico de colimación lineal y rodeado de aire. El análisis de los datos se basa en aproximaciones gaussianas o log-normales a las curvas de distribución de tamaño de las partículas. Para asegurar un correcto procedimiento experimental, los resultados obtenidos al medir un conjunto de muestras de verificación han de coincidir con los valores de referencia. Se obtuvieron resultados precisos para las muestras de verificación, por lo que el procedimiento experimental y el análisis de los datos son correctos. Además aplicamos el método en varias muestras reales, obteniendo resultados válidos en algunos casos. Los casos que arrojaron resultados no válidos se deben a que las condiciones iniciales del modelo no se cumplen. Se necesitaría por tanto información adicional sobre estas muestras para interpretar adecuadamente los resultados. Se sugiere además establecer un modelo de análisis apropiado para materiales que no verifiquen las hipótesis sobre la estructura y forma de las partículas del modelo empleado.

CONTENTS

1. INTRODUCTION

Gracias a los recientes avances en computación, en las últimas décadas la técnica SAXS se ha convertido en una práctica rutinaria principalmente en procesos de síntesis y caracterización de nanomateriales. En SAXS, los ángulos de medición de la intensidad dispersada abarcan de 0.1º a 5º, mientras que las espaciados interplanares que se pueden resolver son de 1 a 100 nm. Para detectar el scattering es indispensable que haya contraste entre la densidad electrónica de las partículas del material de interés y el medio que lo rodea. En términos generales, la intensidad de scattering viene dada por la concentración de partículas, el factor de forma de estas y el contraste. La interpretación de los resultados se basa principalmente en las leyes de Guinier y Porod, así como en el uso de las Transformadas de Fourier.

It has been more than 120 years since the German physicist Wilhelm Conrad Roentgen discovered X-rays while he was investigating cathode-ray tubes. This discovery awarded him the first Nobel Prize in Physics in 1901 at the time that opened a new way of observing materials through the inside. X-rays field has grown to the point that it's an essential tool for multiple scientific disciplines as medicine, astrophysics, industrial production and quality tests, and material characterizations, among others.

This work is focused on the implementation of SAXS technique at SIDIX[1] facilities. SAXS permits the determination of particle systems structure in terms of averaged particle sizes or shapes. This method allows to analyse solid or liquid materials, that may be surrounded by particles of the same or another material (solids, liquids or gaseous) with concentrations between 0.1 – 99.9 wt. %. Structural features can be resolved from 1 to 100 nm (10 to 1000 Å). Typical scattering angles hold from 0.1º to 5º, however these parameters could be extended by measuring in smaller (USAXS)[2] or larger angles (WAXS)[3]. Depending on the optical geometry employed for measuring the scattered intensity, SAXS technique can be differenced in two modes. Transmission mode, for inside material particles; and reflection mode,

[1] SIDIX: Servicio Integrado de Difracción de Rayos X. Universidad de La Laguna.

[2] USAXS: Ultra Small Angle X-ray Scattering

[3] WAXS: Wide Angle X-ray Scattering

for surface-near particles, also called GI-SAXS[4]. We will develop our study under transmission mode, i.e., the incident beam will pass through the bulk material and we will measure the scattered intensity right after the sample. Computer software will help us visualizing the scattered pattern and determining internal features of materials.

In the 1960s SAXS technique was already popular for its capability of size and shape determination of samples. Nowadays, computer processing advances have made SAXS a routine practice in science and industry for material characterization, which usually allows the understanding or finding of physical, chemical and biological properties of interest. Moreover, SAXS permits investigation of live intermolecular interactions such as rearrangement of particles. SAXS applications cover both synthetic and natural materials. Some of them are parts of processes on cosmetics and pharmaceutics, foods and nutrients production, porous materials, synthetic polymers, building materials, minerals, biological nanocomposites and membranes.

1.1. SCATTERING CONDITIONS

X-rays sources wavelength vary from 0.01 to 10 nm. Normally, SAXS sources wavelengths are near to 0.3 nm. In that way, when x-rays hit nanomaterial samples, they widely penetrate the particles. Specifically, the process taking place in this radiation-matter interaction is Thomson Scattering. When incident photons hit the sample (of relatively high atomic number), electrons start oscillating with the incoming radiation wavelength. The result is an outcoming coherent radiation that interferes the detector.

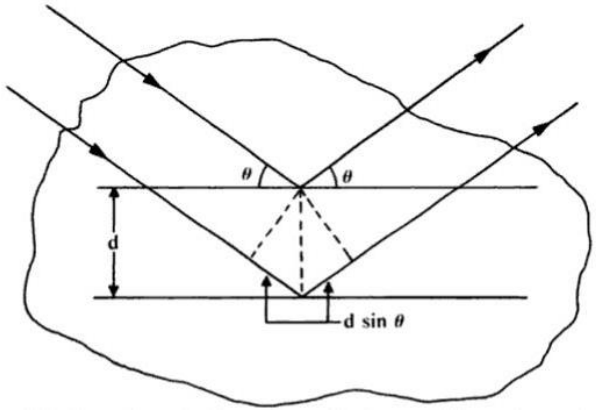

Fig 1. Bragg's law and geometry [2]

$$n\lambda = 2d \sin\theta \quad (1)$$

[4] GISAXS: Grazing incidence SAXS

One of the keys for understanding X-ray diffraction is Bragg's law (Fig 1). It defines the relation between the incident wavelength (λ), the X-rays angle of incidence (θ) and the distance between atomic planes inside the sample (d), being "n" a positive integer. When this equation is satisfied, the scattered intensity occurs in the direction defined by the angle θ. For constructive interference, the path difference must be a multiple of the wavelength. Scattering curves characteristics depend on the internal structure of particle systems such as particle or pore sizes, particle shapes, agglomeration behaviour and more. Consequently, scattering curves can be used for extracting many structural information about materials.

The most relevant material properties for SAXS results are thickness (d), density (ρ), linear absorption coefficient (μ) and scattering cross-section (σ). The scattering cross-section or Thompson factor is the scattered energy produced by an incident radiation of unit energy per unit area. In other words, it's the scattered energy produced by one electron. The direct consequence is that every illuminated electron contributes the same amount of energy to the scattered radiation: the energy of one photon.

$$\sigma = 7{,}93933 \cdot 10^{-26}\, cm^2 \quad (2)$$

Ultimately, scattering efficiency is proportional to the number of electrons illuminated per material volume. For high quality scattering data, samples must have small absorption coefficient (μ), so that they scatter most of the incident radiation.

Regarding imaging sensitivity, scattering has essentially two sources: the sample particles and the matrix material. The matrix material includes the components surrounding the particles of interest, which in our case is the air. In order to make the scattered intensity visible, there must be contrast (difference in electron density, ρ) between the sample material and the matrix material. Naturally, scattering visibility is proportional to the contrast.

Matrix material: ρ_1
Sample material: ρ_2

$$|\Delta\rho| = |\rho_1 - \rho_2| = |\rho_2 - \rho_1| \neq 0 \quad (3)$$

1.2. SCATTERED INTENSITY

SAXS data reduction often requires keeping intensities independent of the wavelength, usually represented in terms of momentum transfer, q.

$$q = \frac{4\pi}{\lambda} \sin\theta \qquad \left(\frac{1}{nm}\right) \quad (4)$$

On the other hand, experimental scattering is made of two components. The background radiation, $I_{M,exp}\,(q)$, which is scattered into all directions and is almost constant at small angles. And the excess scattering, $I_{S,exp}\,(q)$, produced by particles of different material or density which are in the size-range of X-rays. SAXS experiments are focused on detecting this excess scattering component.

To achieve this goal, the background radiation and the dark-count rate of the detector, $I_{dc}(q)$, should be extracted from the sample scattering. The dark-count rate means the averaged intensity that is registered on the detector without any incident beam. It is normally related to thermal processes and is useful to stablish the relevant detection range.

$$\Delta I(q) = \frac{I_{S,exp}\,(q) - I_{dc}(q)}{T_S} - \frac{I_{M,exp}\,(q) - I_{dc}(q)}{T_M} \quad (a.u.) \quad (5)$$

M: matrix material; S: sample material; dc: dark-count rate of the detector; T: transmittance

If the incident beam intensity is $i_o\,(^{a.u.}/_{cm^2})$,[5] the total scattered intensity arriving at the detector is modified by:

$$I_o = i_o\,\sigma\,\frac{A}{R^2}\,T\,[(\sin\varphi)^2 + (\cos\varphi)^2(\cos 2\theta)^2] \quad (6)$$

Being A, the pixel size of the detector; T, sample transmittance; R: sample-detector distance; φ the polarization angle of the incident beam in the detector plane and 2θ the scattering angle.

Because of SAXS experiments conditions, we can make the following approximations:

- X-rays are randomly polarized. Let's take an averaged value of $\varphi \simeq 45º$.
- For SAXS, 2θ is always smaller than 10º. Then, $(\cos 2\theta)^2 \lesssim 1$.

[5] a.u.: arbitrary units

After easy calculations, the intensity arriving at the detector will be:

$$I_o = i_o \, \sigma \, \frac{A}{R^2} \, T \quad (7)$$

The most relevant consequence of equation 7 is that short instruments (on sample to detector distance) have higher efficiency than long instruments.

Regarding sample attributes, the scattering has an important dependence on two solid-state physics concepts: the form factor P(q) related to internal distribution of particles, their size and shape; and the structure factor S(q) associated to particle-particle interactions.

If we recall that detectors measure the squared module of the electric field and considering a sample made of one particle of volume V_1, electron density ρ_1, and form factor P(q)., we get:

$$I \propto |E|^2; \qquad |E| = \rho_1 V_1$$

$$I_1(q) = I_o \cdot \left(\rho_1 V_1\right)^2 \cdot P(q) \quad (8)$$

Furthermore, experimental procedure gives only the contrasted scattered intensity.

$$\Delta I_1(q) = I_o \cdot (\Delta\rho)^2 \cdot {V_1}^2 \cdot P(q) \quad (9)$$

Considering N identical particles and their relative positions, and taking in count the structure factor S(q), the measured scattered intensity results:

$$\Delta I(q) = N \cdot \Delta I_1(q) \cdot S(q) = N \cdot S(q) \cdot I_o \cdot (\Delta\rho)^2 \cdot {V_1}^2 \cdot P(q) \quad (a.u.) \ (10)$$

Direct consequences of this analysis are:

- The intensity scales with the square of the particle volume. For spherical particles the intensity will scale with the six power of the radius. In the final term, the scattering pattern is more sensible to bigger particles in presence of smaller ones.
- The intensity is proportional to the square of the contrast. This eliminates the contrast sign and thus makes voids and points equivalent. That is, the scattered resulting curve produced by a point particle immersed in a matrix will be the same as the one created from a pore inside a material sample. This makes SAXS useful for analysing porous materials but also makes the results ambiguous.

The final scattered intensity of one sample can be summarized into three terms, being K a constant contribution determined by particle contrast, concentration, volume, etc.

$$\Delta I(q) = K \cdot P(q) \cdot S(q) \quad (11)$$

For samples with particles of different size (polydisperse) or different shape (polymorphous), scattering curves will be the sum of their weighted contributions depending on their contrast, particle volume and form factor. In a dilute particle system, scattering contribution of particles are independent, there are no interparticle effects so we can approximate S(q) = 1. The total intensity would result:

$$\Delta I(q) = I_o \sum_{i=1}^{N} \left(\Delta\rho_i\right)^2 {V_i}^2 \cdot P_i(q) \quad (a.u.) \quad (12)$$

Absolute intensity units are not required for the determination of the structure.

1.3. DATA INTERPRETATION

A variety of analysis methods can be used for extracting many internal properties from the scattering features. Here we slightly describe some of the concepts relevant for our calculation method.

1.3.1. Radius of gyration

At small angles, the form factor P(q) can be approximated by a Gaussian curve. Guinier stablished that the curvature of this Gaussian is determined by the "radius of gyration" R_G, related to the overall size of the particle. It can be calculated as the root mean square distance of the object's parts from its center of gravity. This approximation is model independent.

However, if we assume information about the structure or shape of the particle it would be possible to relate particle dimensions with the radius of gyration. Different equations can be derived depending on the assumed particle shape: cylindrical, spherical or lamellar.

1.3.2. Surface per volume

Considering a material composed of spherical particles with radius r, the deduced surface area to volume ratio would be:

$$\frac{S}{V} = \frac{4\pi r^2}{\frac{4}{3}\pi r^3} = \frac{3}{r} \quad (13)$$

Thus, as particle size decreases, a greater portion of particles are found at the surface of a given material compared to those inside. Substances made of nanoparticles have a relative larger surface area when compared to the same volume of the bulk material. Surface area to volume ratio for nanomaterials has a significant effect on their properties. As chemical reactions occur between surface particles, a given mass of nanoparticles will have a greater reactivity than the same amount of material made up of large particles. This means that inert materials in their bulk form become reactive when produced in their nanoparticle form.

In an experimental point of view, Porod defined two general rules applying for scattering patterns.

1- Any scattering profile decays at large scattering angles with K_p/q^4.
   The constant K_p is proportional to the surface per sample volume.
2- Q_P, the second moment of any scattering profile is a universal constant named "the invariant"

Due to instrumental relations between both constants, for line collimation systems (and constants K_L and Q_L) the surface per volume can be approximated as:

$$\frac{S}{V} = 4000 \cdot \pi \cdot \frac{K_L}{Q_L} \cdot \varphi\,(1 - \varphi) \qquad (m^2/cm^3) \quad (15)$$

Being φ the volume fraction of particles. Where K_L is determined from the final slope of $\Delta I(q)$ by fitting $\Delta I(q) \approx \frac{K_L}{q^4} + B$, and Q_P is the first moment of the intensity, $Q_L = \int_0^\infty q\Delta I(q)\, dq \quad (\frac{a.u.}{nm^3})$.

1.3.3. Particle structure

The form factor P(q) of a particle is a curve whose characteristics depend on the particle structure. At small angles, we can see the overall size of the particles by the slope of the form factor. At large angles, the slope of the form factor belongs to the surface properties. In the middle range, the oscillation pattern is due to the particle shape and internal density distribution.

In that way, the domains of a particle form factor are divided in: Guinier, Fourier and Porod's regions.

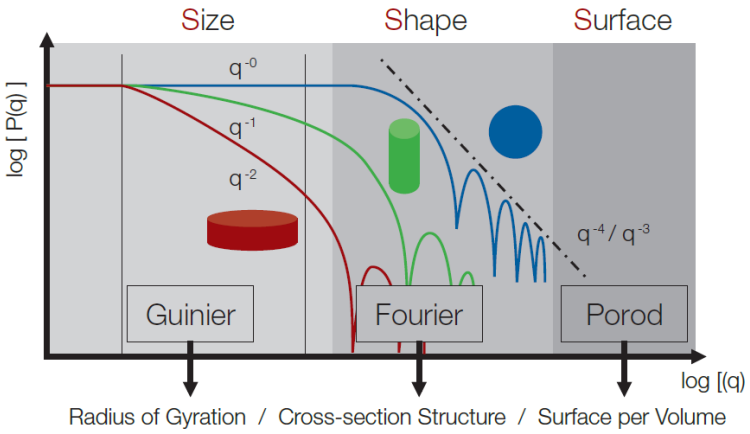

Fig 2. Regions of the form factor in a double logarithmic plot [10]

At small values of q, Guinier's law indicates an initial slope of 0 for spherical particles, of -1 for cylindrical and of -3 for lamellar shape. If the slope is out of these parameters, the particles are larger than the resolution limit and only the Porod region can be observed. At large q-values and according to Porod's law, the scattering curve follows a linear slope of q^{-3} for line collimation and of q^{-4} for point collimation.

The oscillation pattern is a Fourier transformation of the sample. Most detectors only measure the intensity of the Fourier transform, and thus the reconstruction of scattered intensity results in a loose of wave phases information. The direct consequence is we cannot achieve three-dimensional information about samples, so data interpretation becomes complicated.

$$I(q) = 4\pi \int_0^\infty p(r) \frac{\sin(qr)}{qr}\, dr \quad (16)$$

Thus, for extracting information from the Fourier region, its needed to calculate the inverse Fourier transformation into the real space structure. The resulting p(r) curve, PDDF[6], is a histogram of distances that can be found inside the particle, weighted by their electron densities. The distance in which all PDDFs decay to zero indicates the largest distance inside the particle. Core-shell particles and aggregates are easy to identify by their PDDFs.

[6] PDDF: pair-distance distribution function

For centro-symmetric particles, it is possible to rebuild radial density profiles by deconvoluting the PDDFs. Otherwise, additional information and model calculations are required for particles with other symmetries.

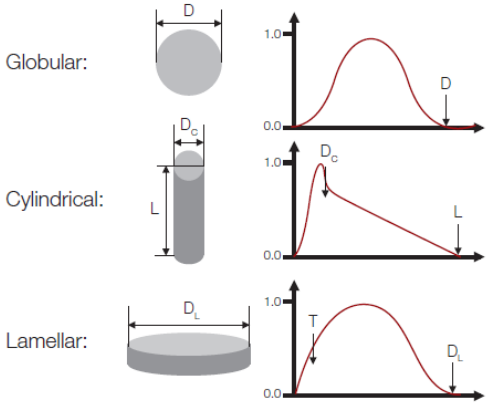

Fig 3. PDDFs profiles for globular, cylindrical and lamellar particle shapes [10]

2. OBJECTIVES

En este trabajo nos centraremos en la implementación de la técnica SAXS en las instalaciones del SIDIX, tomando como referencia unas muestras de verificación proporcionadas por el fabricante del instrumento experimental (PANalytical)

Our objective is to implement Small Angle X-ray Scattering (SAXS) technique in an experimental setup under transmission geometry and line collimation optics. We have used PANalytical Empyrean Diffractometer and PANalytical software. In order to confirm the followed correct methodology, we have analysed three standard samples following *EasySAXS Verification Samples Instructions for use* [6].

3. METHODOLOGY

El equipo instrumental consta de un difractómetro PANalytical y el software proporcionado por el fabricante. Hemos configurado el instrumento teniendo en cuenta que las medidas se hacen a ángulos pequeños muy cerca del haz incidente y que las muestras a analizar están en forma de polvo. Tras el calibrado en incidencia directa, usaremos una programa de medidas común para medir el background y posteriormente las muestras. Para analizar los resultados, aplicaremos un modelo de aproximación gaussiana o log-normal a la distribución del tamaño de partículas.

3.1. INSTRUMENTAL EQUIPMENT AND SOFTWARE

We have used PANalytical Empyrean Alpha 1 Diffractometer, placed at *Servicio Integrado de Difracción de Rayos X* (SIDIX) at Universidad de La Laguna. We configured the instrument in a line collimation system by a series of slits, thus the incident and resulting beam profiles become a well-defined, intense long narrow line.

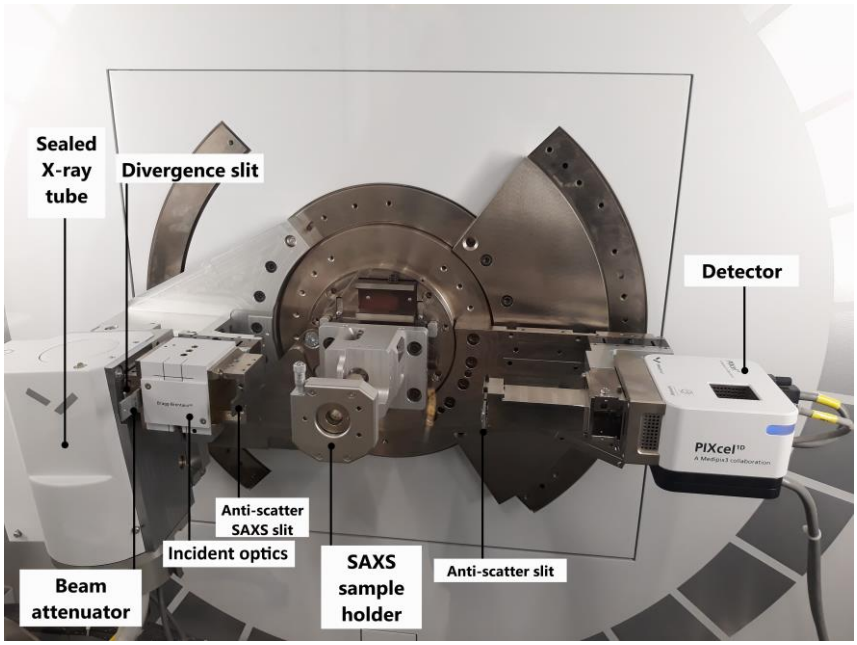

Fig 4. PANalytical Empyrean Alpha 1 Diffractometer parts

The diffractometer source is a polychromatic sealed X-ray copper tube of 45kV and 40mA. The incident optics is a Bragg-Brentano HD module and a monochromator that filters Cu-Kβ component of the copper spectrum so the incident wavelength is Cu-κ_α , which has a wavelength of $\lambda = 1.540598$ Å. Incident optics also contains

a divergence slit of 1/8º and a SAXS anti-scattering slit of 1/32º. A copper beam attenuator of 0.1 mm (mirror/hybrid) avoids the incident beam by hitting directly into the detector and helps differentiating the weak scattering and the incident beam. The sample holder is vertically oriented and placed over a SAXS/WAXS platform.

Finally, the detection system is composed of an anti-scattering slit of 1/16º and a "PIXcel 1D-Medipix3" detector in a receiving slit 0D mode (one channel detection). The sample-detector environment is surrounded by air. We will have to take in mind the detector saturation, which happens at $5x10^6$ cps. The detector sends data into the computer through an electronical system.

The software used is delivered together with hardware. PANalytical Data Collector is for measuring purposes and DataViewer is for plotting SAXS data files. For experimental data treatment, we executed PANalytical EasySAXS V.2.2.0.1158 in a specific analysis program that requires some templates files also included in the package.

3.2. VERIFICATION SAMPLES SET

The verification samples are a set of three samples of non-aggregated nanopowder materials with approximately spherical particle shape, whose maximum particle radius is lower than 50 nm. There is a tendency of primary particles to form agglomerates and the particle size distribution is well defined. This set is meant to verify the correct sample preparation, SAXS measurement and data analysis procedures with EasySAXS.

3.3. EXPERIMENTAL PROCEDURE

3.3.1. Sample preparation

One of the most important features of SAXS technique is that it is non-destructive and requires a minimum sample preparation. In order to get the optimum scattered signal, it's necessary to keep a large and illuminated sample volume. But due to our transmission mode case, we must employ the optimum sample thickness $d_{opt} = \frac{1}{\mu}\ cm$. For sample preparation, we placed and spread a small amount of nanopowder material (approx. 50 mg) between two 6 µm mylar foils (transparent to the X-rays) using the powder holding inserts, the metal pieces of pictures below. In this way the compressed sample results in a thin film.

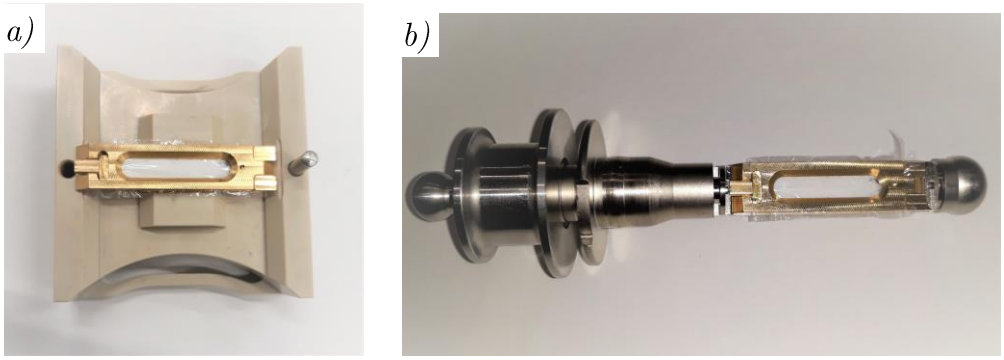

Fig 5. Powder materials preparation.

The preparation tool of a) is used for pressing the sample between mylar foils. After that, we insert the powder holder inside the sample holder of b) and place it on the platform cavity

3.3.2. Zero-incidence angle calibration

The setup of the equipment starts calibrating zero-incidence angle with Data Collector. Angle parameters are Ω as incident angle and 2θ for scattering angle.

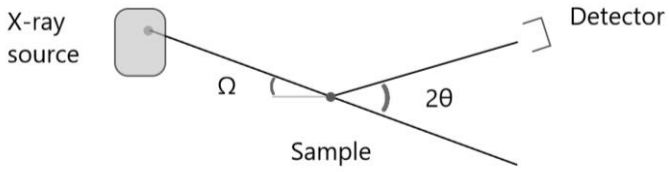

Fig 6. X-rays incident and scattering angles diagram

The calibration consists of the next steps:

1) Put the Diffractometer in the SAXS/WAXS stage
2) Insert the copper attenuator
3) At *incident beam optics* tab, we must configure the beam attenuator to be activated from -10º to 0.05º, that is, while scanning trough the incident beam. After this range, the process stops, and the program requests for manually removing the attenuator. Then, the scanning continues towards higher angles.
4) Rotate the system to Ω= 0º and 2θ = 0º, with Ω_{offset} = 0º. The diffractometer rotates to the position in Fig 4.

5) Perform a "Manual Scan" through the direct beam with the following parameters

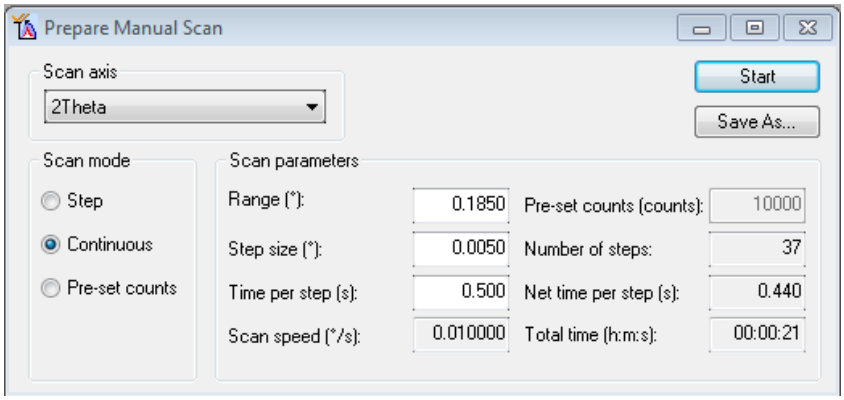

Fig 7. Manual Scan parameters for calibration

6) Check if the resulting scattering curve is centred at 0º in 2θ axis. If it's not, we must redefine zero 2θ position in the centre of the curve under *fine calibration offsets*

7) Repeat the scan for checking the centre of the curve. Then, FWHM[7] must be 0.03 – 0.05 º.

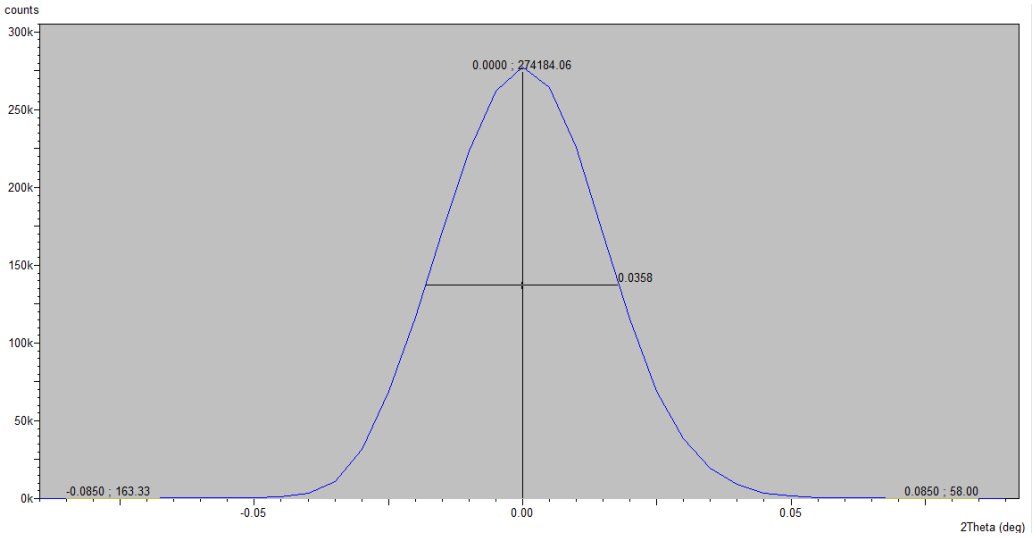

Fig 8. Measured direct beam profile

After redefining the center of the curve we got a FWHM of 0.0358 (Fig 8), which determines an addecuate calibration.

[7] FWHM: Full Width at Half Maximum

3.3.3. Measurements set up

The following background and sample scanning measurements should be done over a common "Absolute Scan program" in Data Collector with the parameters below.

Scan axis	2θ
Scan range	- 0.115º - 5.005º [8]
Step size	0.010º

Table 1. SAXS program parameters using a point detector

This is a requirement for the SAXS data files to be compatible with the analysis templates provided with EasySAXS. Using this set up, measuring times for powder samples will be from 20 to 40 minutes.

3.3.4. Background contribution

The background contribution for this case may come from the sample container, the optical system in the beam path and the air. To identify the background scattering, we measure the scattering of the empty sample holder, mylar foils included, in vertical position. In the analysis step, this contribution will be extracted from all the sample scattering intensities. Often scattering curves present a continuous descending profile, as seen on the background contribution below (Fig 9). Towards larger angles, the intensity decreases quickly.

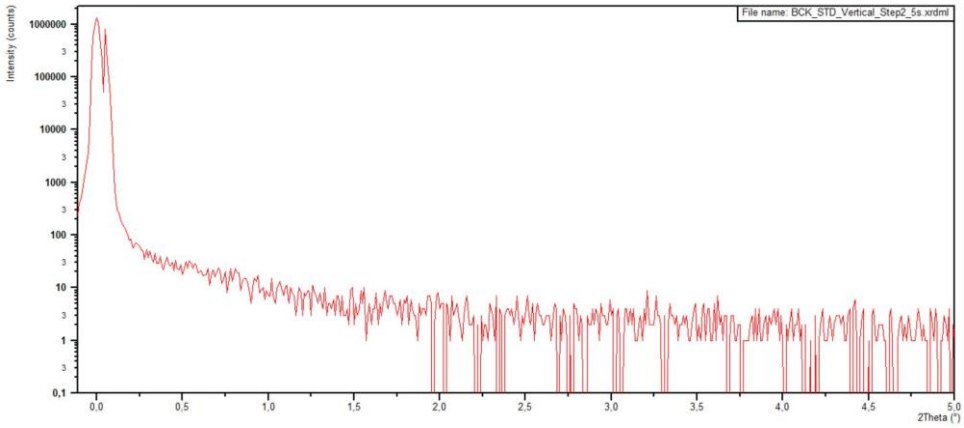

Fig 9. Background scattering obtained

At small angles, the first peak belongs to the attenuated direct beam profile, measured with the attenuator inserted. After this region, the attenuator is removed manually so the intensity comes directly from the sample. By inserting the first data point with attenuator removed (**minimum 2θ = 0.05º**) in the program, this part is removed during the analysis process.

[8] 3.005° end angle for Type 7 scattering curve

3.3.5. Material contribution: absorption coefficient

For material sample measurements we insert the actual sample holder on the SAXS platform and directly run Data Collector with the same configuration. The absorption factor of each sample is the ratio of intensities measured with and without the sample at 0^{o} 2θ. For balancing sample volume and X-ray absorption, obtained absorption values should preferably be between 3 and 5. If any value exceeds significantly this range, we should decrease sample thickness to avoid wrong results.

3.4. DATA ANALYSIS PROCEDURE

Based on the characteristics of as-measured and background-corrected data, [7] defines seven different type of scattering curves. Each definition includes typical size distribution profiles and recommended analysis templates. Depending on the curve type, there are parameter settings that optimize the analysis. On this wise, template files are a pre-programmed sequence of analysis steps. By using templates, it is possible to approximate the size distribution curve by a Gaussian or log-normal function.

For analysing each sample, EasySAXS requests for background file, sample file and template. Therefore, before running the program we should first identify the scattering curve type in order to select the most appropriate template. It is recommended to do the comparison based on the background-corrected curve, although the as-measured curve could be used in many cases. As verification samples are already known, [7] stablishes the appropriate templates as indicated in the next chapter.

The usage of EasySAXS templates will throw reliable results only if all the particles in the sample follow the next assumptions at once: same electron density, essentially homogeneous structure and spherical shape. This condition defines the main limits of the model.

4. RESULTS AND DISCUSSION

Los resultados experimentales de las muestras de verificación se ajustan con bastante exactitud a los valores establecidos por la documentación de referencia. Se consigue por tanto el objetivo esperado, la metodología aplicada es correcta. Como ejemplo de aplicación se miden varias muestras reales y se discuten los resultados. El modelo seguido se basa en hipótesis específicas sobre la estructura de las partículas, por lo que para materiales que se salen de estos parámetros, el modelo no vuelca resultados fiables.

4.1. CONTENTS OF REPORTS

For each analysed sample, the program creates a document report, a size distribution data file in ASCII and a log file with the sequence of analysis steps. All reports contain a compact graph displaying volume-weighted size distribution (D_v) in red, the undersize cumulative in blue and the approximated size distribution function in green. In extended reports the background corrected scattering curve is also shown apart. Reports contain details about data and template files as well as calculated parameters like absorption factor, average particle radius, standard deviation of the distribution and surface-to-volume ratio.

4.2. VERIFICATION SAMPLES RESULTS

The recommended templates for these verification samples are designed for scattering curve types 1 and 2. Type 1 curves are related to samples with “spherical particles or pores with a well-defined size distribution that often can be best approximated by a Gaussian (…). The tendency of primary particles to agglomerate is only moderate” [7]. Moreover, type 2 curves are typical of “spherical particles with a broad size distribution that often can be best approximated by a log-normal function. There could be a tendency of primary particles to agglomerate” [7]. For correct data interpretation of curve types 1 and 2, minor oscillations towards high particle radius in the distribution curves Dv(R) can be neglected in most cases as they have no meaning.

The matching between experimental values and the approximation curve depends on the fulfilment degree on the model considerations, i.e., assumptions on particle structure.

In first place, we checked the absorption factors. As detailed above, the values should preferably be between 3 and 5.

	Experimental absorption factor
Verification sample 1	4.149
Verification sample 2	4.429
Verification sample 3	2.882

Table 2: Experimental absorption factors of verification samples

Samples 1 and 2 fit the ideal range, while sample 3 is slightly below the lower limit. As this is just a recommended range for the experimental absorption factor, we consider the results are appropriate enough and continue the analysis process.

- Verification sample 1

This sample is TiO_2 nanopowder composed of 95% anatase and 5% rutile, with true density of 3.9 g/cm^3. Based on the micrograph in [6], this material has an overall agglomeration tendency and particle radii seem to be very similar.

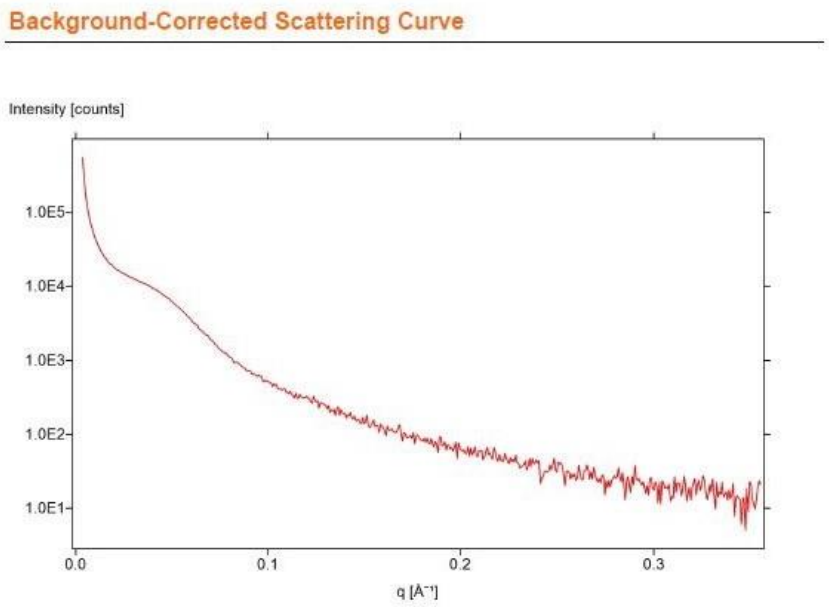

Fig 10. Verification sample 1 background-corrected scattering curve

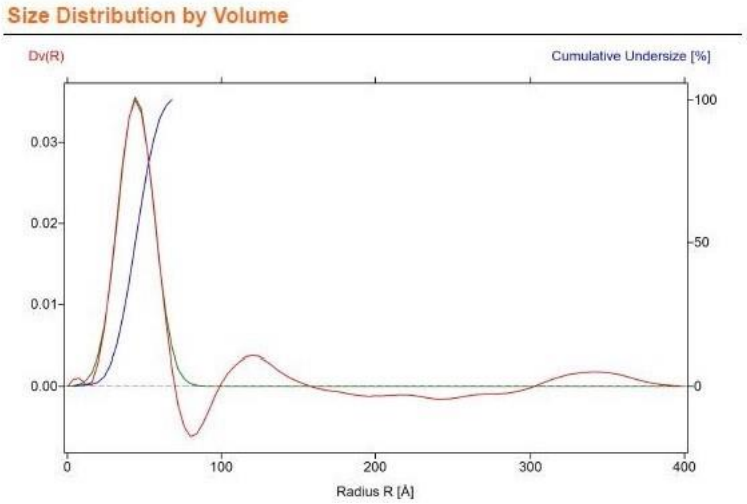

Fig 11. Verification sample 1 size distribution by volume.

The graph shows the volume-weighted size distribution $D_v(R)$ in red, the undersize cumulative in blue and the approximated size distribution function in green.

Results based on Size Distribution by Volume

		Gaussian approximation
Most frequent radius:	44.0 Å	
Average radius:	43.9 Å	
R20:	34.5 Å	34.8 Å
R50:	44.2 Å	44.6 Å
R80:	53.6 Å	54.3 Å
Relative standard deviation:	24.50 %	25.99 %
Surface-to-volume ratio S/V:	0.0751 Å^{-1}	0.0734 Å^{-1}

Fig 12. Verification sample 1 results based on size distribution by volume (left column) and results from the Gaussian approximation (right column)

For analysing this sample, the recommendation is using a gaussian approximation function. As seen on Fig 11 and in the values of Fig 12, the gaussian fits the size distribution curve satisfactorily at the first pronounced peak, also the calculations coincide very accurately. The first peak contains most of the particles inside the sample, whose size distribution is centred on 44 Å. Furthermore, there is a small relative standard deviation of about 25%.

- Verification sample 2

This sample is TiO2 nanopowder composed of 99% anatase, with a true density of 3.9 g/cm3.

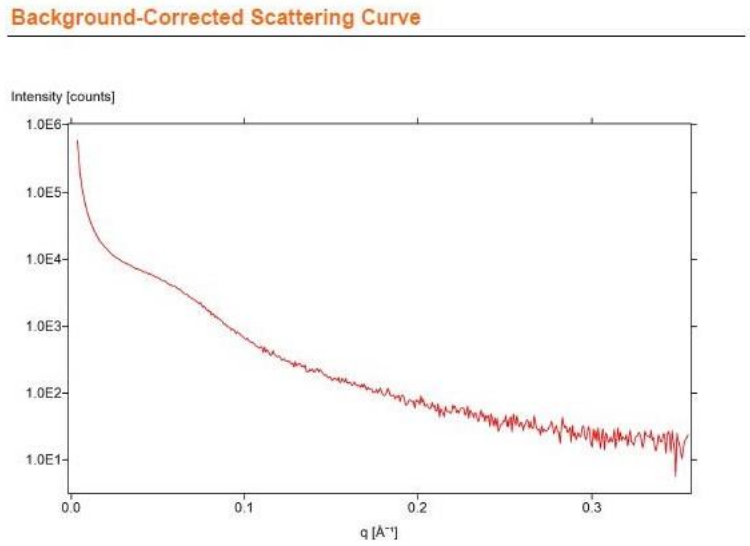

Fig 13. Verification sample 2 background-corrected scattering curve

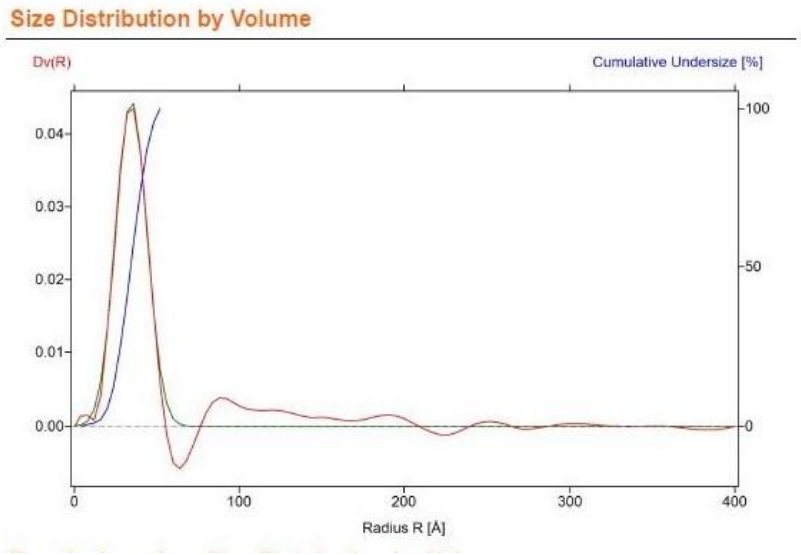

Fig 14. Verification sample 2 size distribution by volume

Results based on Size Distribution by Volume

		Gaussian approximation
Most frequent radius:	36.0 Å	
Average radius:	33.9 Å	
R20:	26.3 Å	26.8 Å
R50:	34.2 Å	34.6 Å
R80:	41.8 Å	42.3 Å
Relative standard deviation:	25.15 %	26.83 %
Surface-to-volume ratio S/V:	0.0975 Å^{-1}	0.0953 Å^{-1}

Fig 15. Verification sample 2 results based on size distribution by volume (left column) and results from the Gaussian approximation (right column)

As this sample composition is very similar to verification sample 1, both size distribution profiles look alike mainly on their first peak. We applied a Gaussian approximation. The results for this material present a range of sizes around 34 Å with a small relative standard deviation of 25%. This material shows a great fitting of Gaussian approximation, which means it is mainly a monodisperse material (uniform in size and shape).

- Verification sample 3

This sample is made of ZnO nanopowder at 99.5% and has true density of 5.6 g/cm^3. Based on the TEM image of [6], this sample has many different particle sizes and shapes with a strong agglomeration tendency although there is a notable presence of holes.

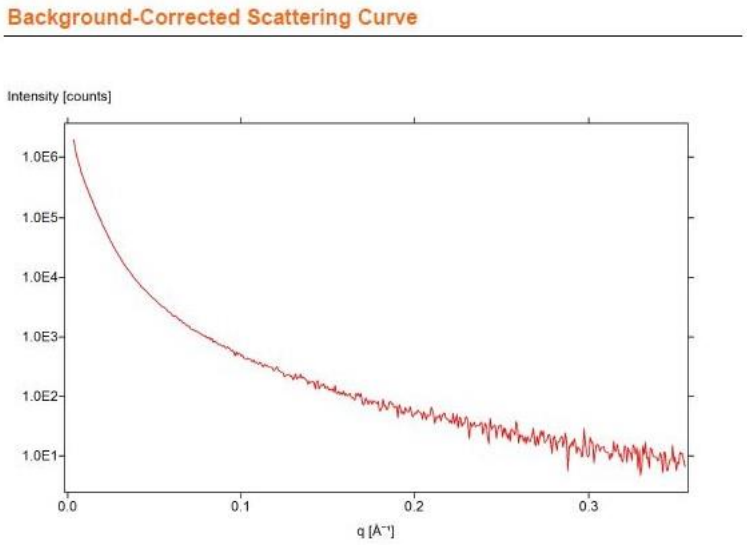

Fig 16. Verification sample 3 background-corrected scattering curve

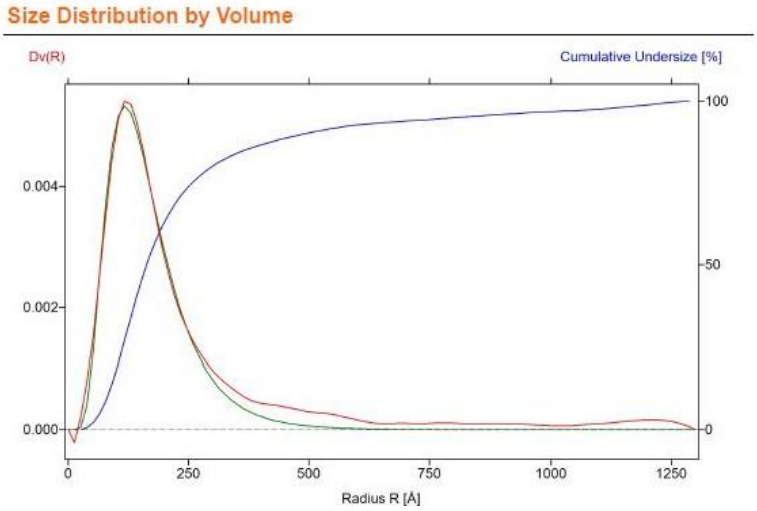

Fig 17. Verification sample 3 size distribution by volume

Results based on Size Distribution by Volume

		Log-normal approximation
Most frequent radius:	117.0 Å	
Average radius:	241.3 Å	
R20:	103.7 Å	98.7 Å
R50:	163.0 Å	148.6 Å
R80:	299.1 Å	223.3 Å
Relative standard deviation:	96.51 %	48.52 %
Surface-to-volume ratio S/V:	0.0207 Å^{-1}	0.0227 Å^{-1}

Fig 18. Verification sample 3 results based on size distribution by volume (left column) and results from the log-normal approximation (right column)

We applied a log-normal approximation function. The size distribution profile shows bigger particle sizes than samples 1 and 2, with a high standard deviation of 96.51%. Meaning a wide variety of particle sizes, whose range is approximately from 100 to 300 Å. The log-normal approximation, however, fits notably with the size distribution curve up to 250 Å.

4.3. DISCUSSION

Based on the preceding reports, we must compare the calculated mean particle radius R50 and the surface-to-volume ratio S/V with the reference values [6]. The experimental process is verified when all the results reproduce these values. As discussed right before, the approximation results can be taken as correct so comparisons will be based on these values for statistical approach. If any value does not fit the limits, for troubleshooting [6] suggests increasing measurement time,

checking the alignment of the diffractometer system or correcting the sample thickness.

	$\mathbf{R50_{ref.}}$ ($\mathbf{Å^{-1}}$)	$\mathbf{R50_{exp.}}$ ($\mathbf{Å^{-1}}$)	**Absolute error =** $\mathbf{\lvert R50_{exp} - R50_{ref.} \rvert}$
Verification sample 1	44.8 ± 2.0	44.6	0.2
Verification sample 2	34.4 ± 0.8	34.6	0.2
Verification sample 3	136 ± 20	148.6	12.6

Table 3: Mean particle radius experimental and reference comparative relation and its absolute error

The results for mean particle radius are satisfactory inside the reference range. If we recall that sample 3 has a relative standard deviation of 48.52%, it explains the magnitude order of the experimental error comparing to samples 1 and 2. In conclusion, R50 obtained values are in concordance with expected.

	$\mathbf{S/V_{ref.}}$ **(Å)**	$\mathbf{S/V_{exp.}}$ **(Å)**	**Absolute error =** $\mathbf{\lvert S/V_{exp.} - S/V_{ref.} \rvert}$
Verification sample 1	0.0734 ± 0.0040	0.0734	0
Verification sample 2	0.0978 ± 0.0070	0.0953	0.0025
Verification sample 3	0.0243 ± 0.0040	0.0227	0.0016

Table 4: Surface-to-volume ratio experimental and reference comparative relation and its absolute error

For the surface-to-volume ratio, the three values are also inside the experimental error, hence the results fit accurately enough the theoretical values.

By following the experimental procedure, the indicator parameters R50 and S/V have been reached. Thus, we can verify the methodology for SAXS: measurement conditions and data analysis procedure. In this way, we have successfully reached our main objective. Consequently, future SAXS experiments made according to this method will throw correct results.

4.4. APPLICATION EXAMPLES

We measured a series of nanomaterial samples in order to reproduce experimental routines and data analysis. As these were unknown materials, we needed to plot their SAXS data curves to identify their scattering curve type. Then, we opened the associated template and executed EasySAXS program as described before.

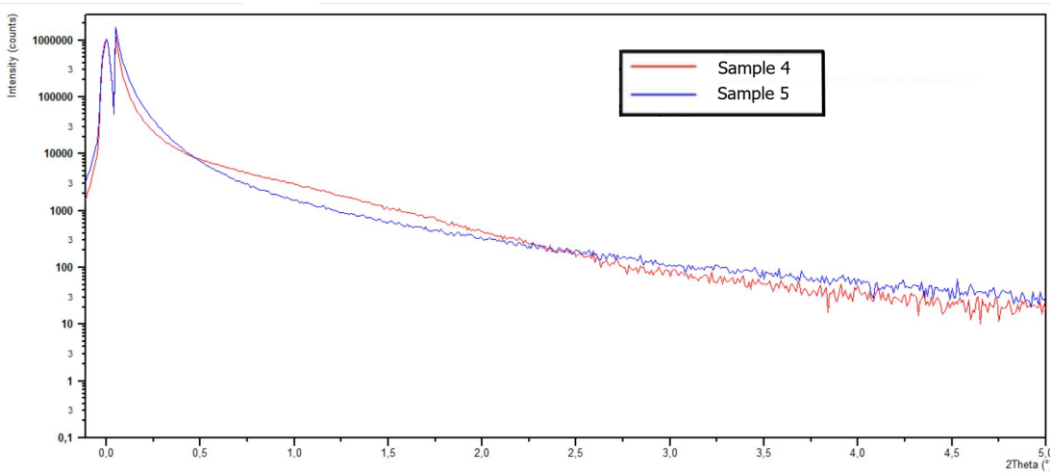

Fig 19: As-measured scattering curves of samples 4 and 5

From the six measured materials, here we will discuss two representative samples, named sample 4 and sample 5. Their background-corrected scattering curves (Fig 19) look like type 4 scattering curves which are typical of "spherical particles or pores with probably a well-defined size distribution. The average radius is probably below 20 nm (200 Å). The tendency of primary particles to agglomerate is relatively strong." [7]. For both samples we applied log-normal approximations.

For us to start the discussion of results it is important to take in count that SAXS averages the illuminated sample volume structure. This makes the results ambiguous and thus sometimes creates the need of complementary information in order to interpret data.

	Absorption factor
Sample 4	1.308
Sample 5	1.233

Table 5: Experimental absorption factors for samples 4 and 5

First, the obtained absorption factors are around 1.3, which are values lower than the ideal range. However, as discussed above, the data quality is enough for this experimental data and thus we consider this absorption values acceptable.

- Verification sample 4

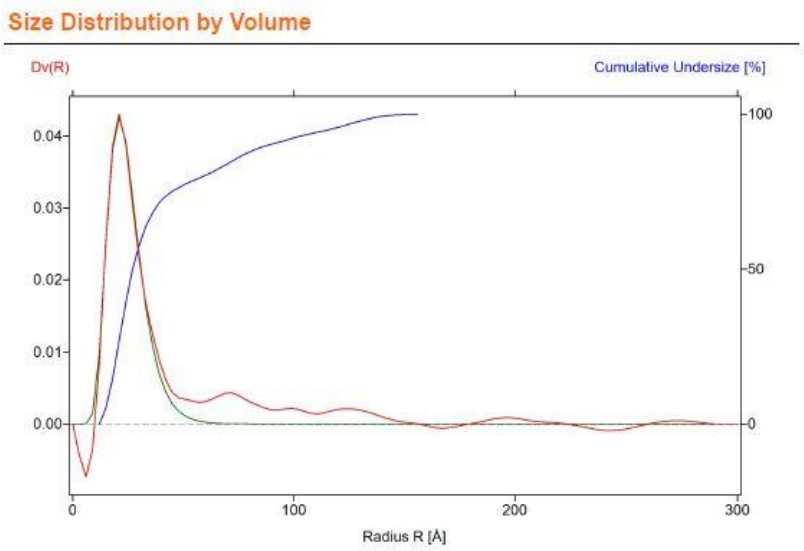

Results based on Size Distribution by Volume

		Log-normal approximation
Most frequent radius:	21.0 Å	
Average radius:	39.9 Å	
R20:	19.3 Å	17.7 Å
R50:	27.1 Å	23.4 Å
R80:	59.1 Å	30.7 Å
Relative standard deviation:	76.40 %	32.69 %
Surface-to-volume ratio S/V:	0.1091 Å^{-1}	0.1354 Å^{-1}
Absorption factor of sample:	1.308	

Fig 20. Sample 4 report extract

For type 4 curves, [7] indicates that the long tail of Dv(R) towards larger radii is insignificant, so we can neglect it for interpretation of results. Thus, the approximated results are more reliable than the results obtained from the original Dv(R). Furthermore, the most frequent radius will be estimated correctly, while R50, R20 and R80 are likely to be overestimated and finally S/V will be underestimated.

The graph on Fig 20. shows a very great fitting of the log-normal function around the main peak. Consequently, the approximated results can be taken as correct. Following the indications above, the most frequent radius of 21 Å is reliable. Also, the over and underestimations of values follow the expected behaviour. The approximated relative standard deviation of 32.69 % means that the main particle sizes are close. In conclusion, the sample is made of spherical

particles with well-defined size distribution, the mean particle radius is 23.4 Å and the surface-to-volume ratio is 0.1354 $Å^{-1}$. In that way, sample 4 performs accurate results that bring information about its internal structure.

As complementary information, TEM[9] images of this sample composition at different scales confirm approximately spherical particles with similar sizes and a moderate agglomeration tendency.

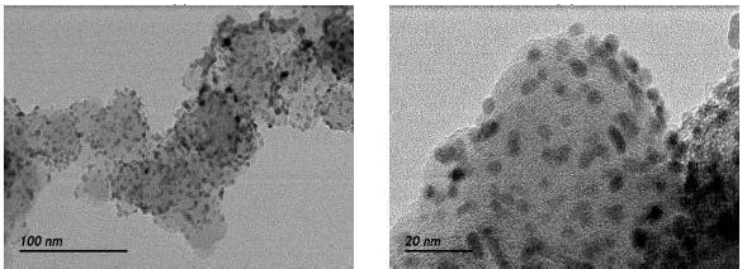

Fig 21. Microscopy images of sample 4 material at different scales [9]

- Other satisfactory cases

Two other real samples presented great fitting on their approximations at the first peak, thus the approximated results of the analysis can be taken as correct. Fig 22 shows the reports obtained for these cases. For the sample on the left the resulting mean particle radius is 11.2 Å while the sample on the right presents a value of 23.4 Å.

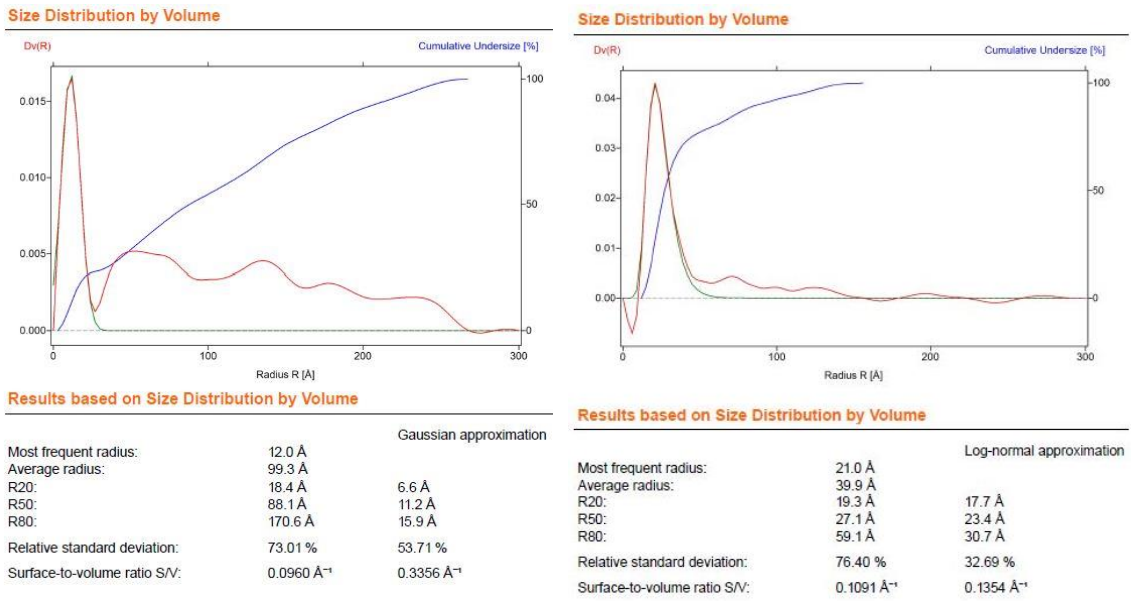

Fig 22. Samples cases with great fitting and correct analysis results

[9] TEM: Transmission electron microscopy

- Verification sample 5

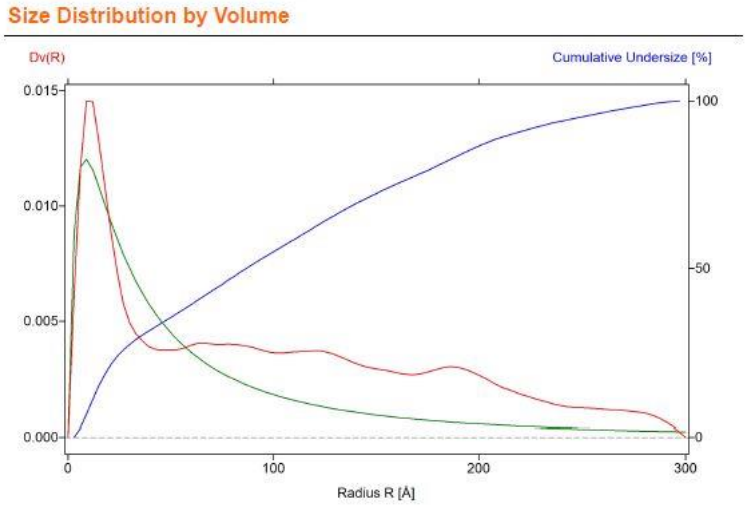

Results based on Size Distribution by Volume

		Log-normal approximation
Most frequent radius:	9.0 Å	
Average radius:	100.2 Å	
R20:	19.4 Å	14.5 Å
R50:	86.7 Å	42.6 Å
R80:	177.4 Å	124.5 Å
Relative standard deviation:	77.91 %	127.79 %
Surface-to-volume ratio S/V:	0.0971 Å^{-1}	0.1546 Å^{-1}
Absorption factor of sample:	1.233	

Fig 23. Sample 5 report extract

The distribution curve of sample 5 covers a broad radius range of 0 – 300 Å. This makes the average radius (100.2 Å) to be remarkably separated from the most frequent radius (9.0 Å). In that way, the log-normal approximation does not fit the experimental curve and consequently the approximated calculations are not reliable. Only R20 values approximately agree due to the main peak strong definition.

The quantitative results do not coincide because the sequence of calculation steps of the templates is not designed for particles with these characteristics. Furthermore, this behaviour wouldn't improve using a much more different curve type. This material clearly does not hold a well-defined particle size neither a homogeneous structure, i.e., it does not reach the analysis assumptions.

Thus, in this case, the model we are using is not the most appropriate procedure for extracting information. Only qualitative information can be used for interpreting some sample characteristics. In conclusion, sample 5 does not work for this method hence the obtained values are not accurate.

- Other unreliable cases

Two other real samples presented excessively inadequate fitting of the resulting curves and thus put in evidence the necessity of different analysis models. The reports for these samples are shown at Fig 24.

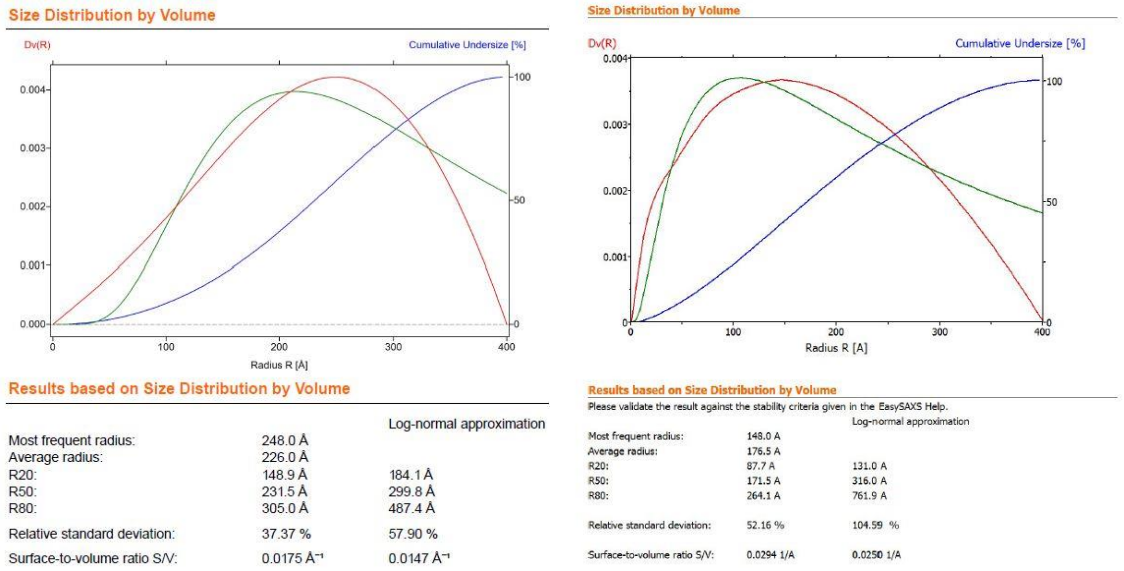

Fig 24. Samples cases with inadequate fitting and unreliable analysis results

5. CONCLUSSION

La técnica SAXS es un método ideal para obtener de forma sencilla información estructural de nanomateriales. Dada la ambigüedad intrínseca de los resultados, combinando esta técnica con microscopía se pueden interpretar los datos y obtener una imagen completa de muestras desconocidas. Futuros trabajos podrían centrarse en aplicar la técnica a distintos tipos de materiales así como en diseñar modelos de análisis para sistemas de partículas inhomogéneas con formas no esféricas.

We have successfully implemented SAXS at SIDIX facilities, by accurately reproducing reference parameters of a verification samples set. In addition, the method works for many of the real samples studied. As evident from the previous discussion, SAXS is an ideal technique for finding structural information of nanoscale particle materials using simple experimental configuration and analysis process. In situ experiments, non-destructivity of samples, many different material

natures allowed, and relatively short measurement times are some of SAXS measurement process advantages. Furthermore, a setup in air already gives proper performance.

Local structure details are not visible by this technique unless they are representative all over the sample volume. On the other hand, there is a loose of phase information of the Fourier transform that sums up to the ambiguity of data. Thus, the main challenge of SAXS is data interpretation. Normally, SAXS results are complemented by additional sample information such as micrographs for correct data interpretation.

In general, for SAXS data quality improvement the absorption factor of samples could be optimized. For materials with non-spherical particle shapes, different particle sizes or different agglomeration levels it would be necessary the modelling of specific analysis steps since the followed methodology cannot reach reliable results. Finally, future studies could be focused on using the same experimental configuration for analysing solid objects, liquids, fibers or mesoporous materials.

6. REFERENCES

[1] Babić, R. R., Stanković-Babić, G., Babić, S. R., & Babić, N. R. (2016). *120 years since the discovery of x-rays.* Medicinski pregled, 69(9-10), 323-330.

[2] Blakemore, J. (1985). *Solid state physics* (2nd rev. ed.). Cambridge: University Press.

[3] Guinier, A., Fournet, G. *Small-Angle Scattering of X-rays* (1955) Wiley, New York

[4] Laggner, P., Kratky, O., Kostner, G., Sattler, J., & Holasek, A. (1972). *Small angle X-ray scattering of LpA, the major lipoprotein family of human plasma high density lipoprotein HDL3.* FEBS letters, 27(1), 53-57.

[5] Pauw, B. R. (2011). *How to do a perfect SAXS measurement.*

[6] PANalytical B.V., The Netherlands, 2010 *EasySAXS Verification Samples. Instructions for Use.* (2nd ed.)

[7] PANalytical B.V., The Netherlands, 2014 *EasySAXS Quick Start Guide.* (3rd ed.)

[8] PANalytical B.V., The Netherlands, 2010 *SAXS/WAXS Application Guide for the Empyrean and X'Pert PRO MPD platforms*

[9] Rivera Gavidia, L. M., Sebastián, D., Pastor, E., Aricò, A. S., & Baglio, V. (2017). *Carbon-Supported Pd and PdFe Alloy Catalysts for Direct Methanol Fuel Cell Cathodes.* Materials (Basel, Switzerland), 10(6), 580. doi:10.3390/ma10060580

[10] Schnablegger, H. and Singh, Y., (2013). *The SAXS guide: getting acquainted with the principles (3rd ed).* Austria: Anton Paar GmbH.

[11] Vachette, P., & Svergun, D. I. (2000). *Small-angle x-ray scattering by solutions of biological macromolecules*